ISBN: 978-3-95450-227-1 ISSN: 2673-5490 doi:10.18429/JACoW-IPAC2022-MOPOST030

PROTON IRRADIATION SITE FOR Si-DETECTORS AT THE BONN ISOCHRONOUS CYCLOTRON

D. Sauerland,*R. Beck, P.D. Eversheim, Helmholtz-Institut f.Strahlen- u. Kernphysik, Bonn,Germany
J. Dingfelder, P. Wolf, Silizium Labor Bonn, Physikalisches Institut, Bonn, Germany

Abstract

The Bonn Isochronous Cyclotron provides proton, deuteron, alpha particle and other light ion beams with a charge-to-mass ratio Q/A of $\geq 1/2$ and kinetic energies ranging from 7 to 14 MeV per nucleon[1]. At a novel irradiation site, a 14 MeV proton beam with a diameter of a few mm is utilized to homogeneously irradiate silicon detectors, so-called devices under test (DUTs), to perform radiation hardness studies. Homogeneous irradiation is achieved by moving the DUT through the beam in a row-wise scan pattern with constant velocity and a row separation smaller than the beam diameter. During the irradiation procedure, the beam parameters are continuously measured non-destructively using a calibrated, secondary electron emission-based beam monitor, installed at the exit window of the beamline. The diagnostics and the irradiation procedure ensure a homogeneous irradiation with a proton fluence error of smaller than 2 %. In this work, an overview of the accelerator facility is given and the irradiation site with its beam diagnostics is presented in detail.

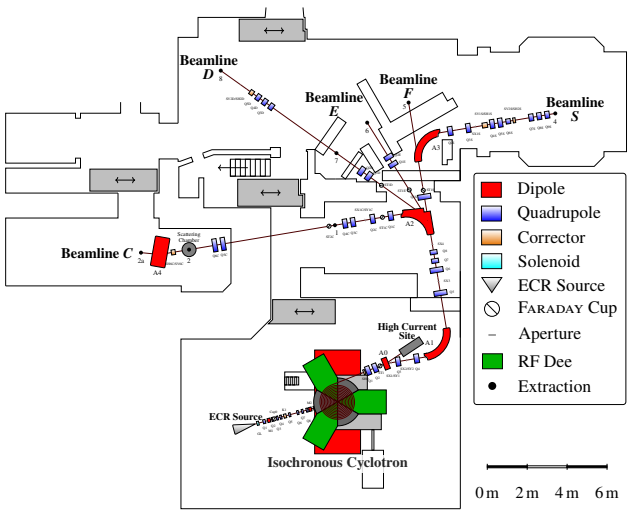

Figure 1: Overview of the accelerator facility.

BONN ISOCHRONOUS CYCLOTRON

The accelerator facility of the Bonn Isochronous cyclotron is shown in Fig. 1. Here, light ions, like protons, deuterons or alpha particles with a kinetic energy of 7 to 14 MeV/A, are provided to five experimental sites. The ions are generated by two external electron cyclotron resonance (ECR) sources.

* sauerland@hiskp.uni-bonn.de

[1] Operating at the third cyclotron harmonic ($h = 3$). For the acceleration of heavier ions up to $^{16}O^{6+}$, see Fig. 2.

Table 1: Parameters of the Bonn Isochronous Cyclotron

available ions	p, d, α, …, $^{16}O^{6+}$
energy ($h = 3$, $Q/A \geq \frac{1}{2}$)	7 to 14 MeV/A
beam current (ext.)	$\lesssim 1\,\mu A$
injection / extraction radius	38 mm / 910 mm
number of revolutions	approx. 120
hill sectors	3 × 40°, 0° spiral angle
hill / valley field strength	1.9 / 0.7 T (max.)
flutter factor	0.62
dees	3 × 40°, 40 kV (max.)
cyclotron harmonic h	3, 9
RF frequency ν_{RF}	20.1 to 28.5 MHz
hor. / vert. emittance	16 / 22 mm mrad
relative energy spread	4×10^{-3}

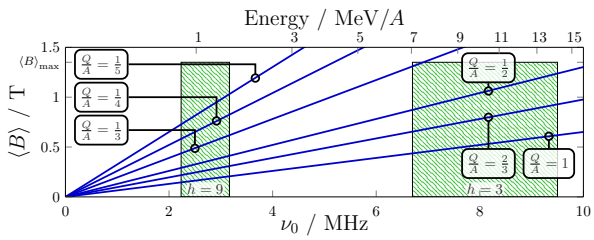

Figure 2: Parameter space of possible cyclotron operation (green) with average magnetic flux density $\langle B \rangle$ and ν_0.

A two-stage 5 GHz source is located beside, whereas a single-stage, polarized 2.5 GHz source is situated underneath the cyclotron. The generated 2 to 8 keV beam is guided below and is injected vertically into the cyclotron's magnetic center using an electrostatic hyperboloid inflector.

The Bonn Isochronous Cyclotron [1] is an isochronous AVF cyclotron with a 120°-symmetric magnetic field configuration in the azimuthal plane. Its magnet yoke therefore is separated into three hill-and-valley sectors with 0° spiral angle. In the valleys, three broadband dees are located, providing an acceleration voltage of up to 40 kV. The main parameters of the cyclotron are shown in Table 1. Due to its symmetry, the cyclotron normally operates at the third cyclotron harmonic $h = 3$, where the RF frequency ν_{RF} equals three times the ions' cyclotron frequency ν_0, but also an operation at $h = 9$ is possible. The RF frequency range and the maximum average magnetic flux density $\langle B \rangle_{max}$ of approx. 1.4 T define the cyclotron's mass-to-charge acceptance, as shown in Fig. 2. After approx. 120 revolutions, the beam is extracted to a field-compensated channel in a single-turn extraction, using an electrostatic septum. The

ISBN: 978-3-95450-227-1 ISSN: 2673-5490 doi:10.18429/JACoW-IPAC2022-MOPOST030

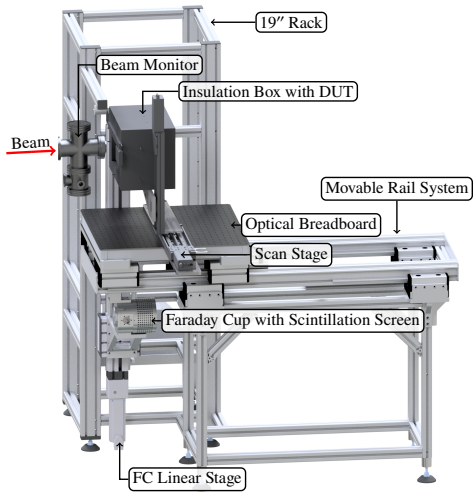

Figure 3: CAD render of the irradiation site.

extracted beam can either be guided to the high current site, used to produce induced radioactivity in target material, or it is transported to the experimental sites via the high-energy beamline [2].

IRRADIATION SITE

In the *C* beamline, at extraction 2a (comp. Fig. 1), a new site for proton irradiation of silicon detectors has been installed. The site is shown in Fig. 3. A beam monitor, situated directly upstream of the beam exit window, is used for non-destructive, continuous beam diagnostics. The experimental setup is positioned on an optical breadboard in front of the window, which itself is mounted on a rail system with a supporting structure made of aluminum profiles. The rail system allows retracting of the experimental setup along the beam axis, enabling to position an in-house developed Faraday cup (FC) in front of the exit window, using a vertical linear stage. The FC is used to calibrate the beam monitor and features a *Chromox* scintillation screen for visual beam diagnostic. The site is complemented by a 19″ rack for installation of the readout electronics as well as other devices and providing external interfaces to the irradiation site.

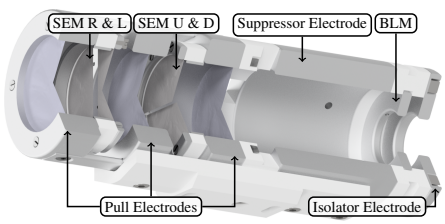

Figure 4: CAD render of a sectional view of the beam monitor with SEM (left) and BLM module (right).

Beam Monitor

The custom-made beam monitor, comprising a secondary electron monitor (SEM) module and a beam loss monitor (BLM) module, is shown in Fig. 4. In the SEM module, the surface emission of low-energy secondary electrons (SE), upon impact of fast ions into matter, is used to measure the beam current and position. Here, the beam penetrates two 5 µm-thick, carbon-coated[2] Al foil pairs, successively seg-mented vertically (SEM R & L) and horizontally (SEM U & D). Removing the emitted SE from the electrically-isolated SEM-foils, results in a current flowing onto the foils which is proportional to the incident ion beam current. Therefore, pull electrodes are located in close proximity to each SEM-foil's surface, consisting of three 5 µm-thick Al foils, biased with +100 V. The sum of all foil currents allows for online beam current measurement after calibration whereas the seg-mentation enables to determine the relative beam position. The BLM module consist of a 3 mm-thick Al iris with a diameter of 20 mm, mimicking the dimensions of the exit window, as well as a two suppressor electrodes positioned in front of and behind the iris. Upon ion impact on the BLM iris, a current is flowing, indicating beam-truncation at the exit window. To prevent charge-loss due to SE emission, the suppressor electrodes are biased with −100 V. Using the information provided by the BLM as well as the cal-ibrated SEM, the beam monitor enables to determine the actual beam current which is extracted to the irradiation site. The beam monitor design is based on studies utiliz-ing the Electrostatic and Particle in Cell (PIC) Solver of CST Studio Suite to maximize the SE col-lection from the SEM-foils. A scenario with a 13.6 MeV proton beam is shown in Fig. 5. Here, SE trajectories are simulated, based on the potential of the electrodes and the SE-generated space charge. The SE yield (SEY) due to pro-ton impact is calculated on basis of measurements of [3]. According to [4], the downstream SEY is approx. twice as large as upstream, for high-energy protons. The SE emission energy probability density function is a gamma distribution with an estimated mean energy of 15 eV, based on measure-ments of [5]. For this scenario, the resulting SE collection efficiency for both SEM-foils is $(99.11 \pm 0.19)\%$ (upstream) and $(99.77 \pm 0.04)\%$ (downstream).

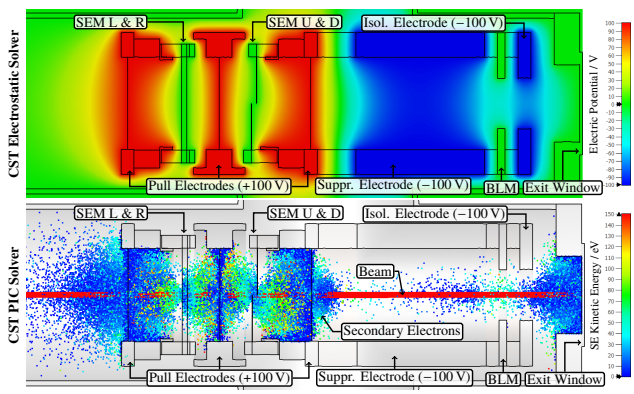

Figure 5: CST simulations: Electric potential of the beam monitor (top). Spatial distribution of SE for a proton beam current of 1 µA in its equilibrium state (bottom).

[2] To anticipate surface carbonization in vacuum with time, ≈ 70 nm layer thickness

ISBN: 978-3-95450-227-1 ISSN: 2673-5490 doi:10.18429/JACoW-IPAC2022-MOPOST030

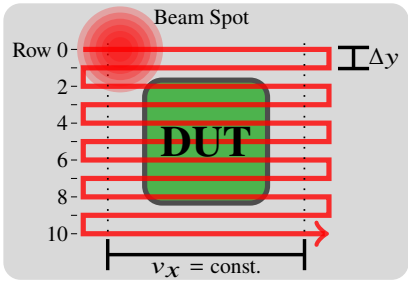

Figure 6: Relative movement of the beam along the scan pattern over the DUT (green) and the shielding (gray).

IRRADIATION AT THE CYCLOTRON

A 14 MeV proton beam is used to irradiate DUTs, housed in a thermally-insulated cooling box (comp. Fig. 3). The box fits DUTs with a maximum size of $19 \times 11\,\mathrm{cm}^2$ and is mounted on a scan stage, which has a range of $30 \times 30\,\mathrm{cm}^2$. Typically, DUTs are mounted behind a dedicated, 6 mm-thick Al shielding, exposing only the DUT to the beam. A scintillation screen on the shielding allows for an optical, beam-based alignment of the setup. To prevent annealing during irradiation, nitrogen gas is guided through a liquid nitrogen reservoir and onto the DUT, retaining a temperature of $< -20\,°\mathrm{C}$. To perform a homogeneous irradiation, the scan stage is used to move the DUT through the beam in a row-wise scan pattern (see Fig. 6).

DAQ and Control

A custom-made analog readout board is used to linearly convert the current signals from the beam monitor and FC to voltages ranging from 0 to 5 V. To resolve different magnitudes of currents, the board features several gain settings, corresponding to input current scales between 50 nA to 100 µA. A *Raspberry Pi* single-board computer, utilizing an analog-to-digital extension board, is used to digitize the voltage signals and interface as well as to control the components of the irradiation setup. The *Python* package `irrad_control`[3] is a graphical user interface-based control and DAQ software, allowing to operate the irradiation site and experimenters' setup from the facility's control room. During irradiation, it provides continuous analysis and monitoring of the applied proton fluence, DUT temperature and beam parameters.

Beam-Driven Irradiation Procedure

To ensure a homogeneous fluence distribution, a row-wise scan pattern is constructed, on which the DUT is moved through the proton beam repeatedly (see Fig. 6). By providing a constant velocity v_x, when traversing the DUT, and a row separation Δy smaller than the beam diameter, the beam's transversal charge distribution is unfolded homogeneously onto the DUT. Therefore, an area larger than the DUT is scanned, with turning points located off the DUT, on the shielding. The irradiation procedure is carried out autonomously and is beam-driven, adapting to changing beam conditions to maximize homogeneity. At turning points, beam parameters are probed against predefined requirements (e.g. current, stability, position) and consequently, the scan is adapted or paused until conditions suffice.

Fluence Distribution and Error Estimation

Continuous measurement of the extracted beam current during irradiation allows to generate a map of the applied fluence on the scan area. A typical fluence distribution is shown in Fig. 7. In the central region, containing the DUT, the fluence is applied homogeneously. In contrast, the turning point regions, located at the opposite ends of the area, are exposed to a higher fluence due to the turning itself as well as pausing, initiated by the beam-driven irradiation procedure. The variance of the proton fluence within the homogeneous region is insignificant with respect to the its relative uncertainty of $\leq \sqrt{3}\%$. It is composed of the individual error on the beam monitor calibration and the readout board accuracy.

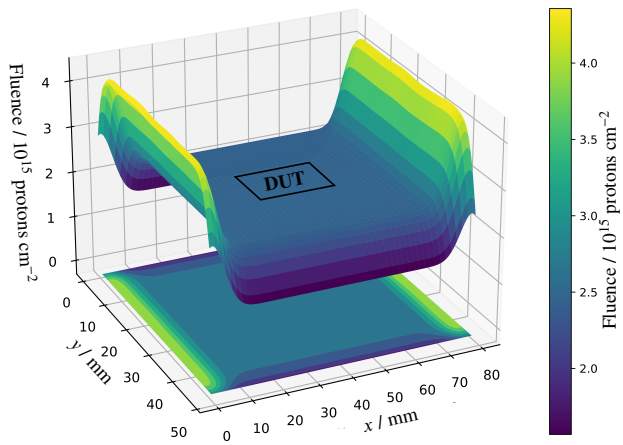

Figure 7: Typical fluence distribution on the scan area for a DUT aim fluence of $2.5 \cdot 10^{15}$ protons cm^{-2}.

REFERENCES

[1] "The AEG Isochronous Cyclotron at the University of Bonn", *IEEE Trans. Nucl. Sci.*, vol. 13, pp. 435 - 436, 1966. doi:10.1109/TNS.1966.4324267

[2] F. Hinterberger et al., "The Beam Handling System at the Bonn Isochronous Cyclotron", *Nucl. Instrum. Methods,* vol.130, 1975. doi:10.1016/0029-554X(75)90033-6

[3] H.P. Beck, R. Langkau, "Die Sekundärelektronen-Ausbeute verschiedener Materialien bei Beschuß mit leichten Ionen hoher Energie", *Zeitung für Naturforschung A*, Vol. 30(8), (1975)

[4] E.F. Da Silveira, J.M.F. Jeronymo, "Secondary Electron Emis-sion from the Entrance and Exit Surfaces of Thin Aluminium Foils under Fast Light Ion Bombardment", *Nucl. Instrum. Methods Phys. Res., Sect. B*, vol. 24-25, 1987. doi:10.1016/0168-583X(87)90702-6

[5] H. Rothard, K.O. Groeneveld, J. Kemmler, "Kinetic Electron Emission from Ion Penetration of Thin Foils in Relation to the Pre-Equilibrium of Charge Distributions", *Particle Induced Electron Emission II*, Springer Verlag, 1992

[3] Source code at `https://github.com/SiLab-Bonn/irrad_control`